ACS OMEGA

Open Access

http://pubs.acs.org/journal/acsodf

Article

Exploring the Target Genes of Fucosylated Chondroitin Sulfate in Treating Lung Adenocarcinoma Based on the Integration of Bioinformatics Analysis, Molecular Docking, and Experimental Verification

Nana Li, Xinhong Zhu, Hua Zhang, Xiaohui Yang, Mingju Shao, Shichao Cui, and Cunzhi Lin*

Cite This: *ACS Omega* 2024, 9, 46312−46322

Read Online

ACCESS | Metrics & More | Article Recommendations

ABSTRACT: Fucosylated chondroitin sulfate (FCS), extracted from sea cucumbers' body walls, has been found to inhibit the proliferation of lung adenocarcinoma (LUAD) cells. However, there have been few studies of the associated drug targets. This study combined bioinformatics analysis and molecular docking to screen the main targets of FCS intervention in LUAD. Moreover, an experimental validation was performed. First, we downloaded the LUAD gene data set from The Cancer Genome Atlas (TCGA) database and the cisplatin (DDP) resistance gene data set of LUAD A549 cells from the Gene Expression Omnibus (GEO) database. Nine significant genes (PLK1, BUB1, CDK1, CDC20, CCNB1, BUB1B, KIF11, CCNB2, and DLAGP5) were identified by bioinformatics analysis, and these nine genes overlapped in both data sets. Then, molecular docking results showed that FCS had a better affinity with target proteins BUB1 and PLK1. Further experimental verification revealed that FCS inhibited the growth of A549 cells and increased the sensitivity of A549 cells to DDP. Quantitative real-time polymerase chain reaction (qRT-PCR) revealed that A549 cells treated with FCS exhibited down-regulated BUB1 and PLK1 mRNA expression. At the same time, FCS+DDP treatment resulted in a more significant reduction in BUB1 and PLK1 mRNA expression than DDP or FCS treatment alone. These findings reveal potential targets of FCS for LUAD and provide clues for the development of FCS as a potential anticancer agent.

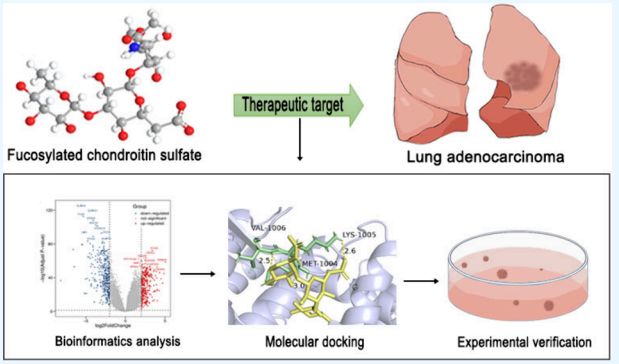

INTRODUCTION

Lung cancer is currently the most common cause of death in people with malignant tumors worldwide, with a five-year survival rate of less than 20%.[1,2] Adenocarcinoma is the most common lung cancer subtype, accounting for around 50% of all lung cancer cases, with yearly increases being observed in its frequency.[3] Lung adenocarcinoma (LUAD) rarely has obvious clinical symptoms in the early stages, meaning that most patients are diagnosed at an advanced stage.[4] Despite the emergence of new therapies, such as molecularly targeted therapy and immunotherapy, chemotherapeutic agents such as cisplatin (DDP) remain the classic and most frequently applied treatment.[5] However, innate or acquired resistance to DDP treatment is common.[6]

Small molecule compounds found in natural products have traditionally served as a valuable source for drug development.[7,8] In this regard, there are two main types of sea cucumber polysaccharides: fucosylated chondroitin sulfate (FCS) and fucoidan.[9,10] A number of studies have suggested that FCS may exert anticancer effects.[11] Indeed, in addition to lung cancer,[12] FCS inhibits the adhesion and invasion of renal cancer cells, inhibits breast cancer cell metastasis.[13,14] Furthermore, FCS exhibits antiangiogenic, anticoagulant, and anti-inflammatory effects.[15,16] Based on such findings, FCS may be an ideal therapy for the management of cancer, although the lack of a comprehensive understanding of its functional mechanism has hindered drug development.

Bioinformatics methods are widely utilized in the field of molecular biology and recognized as a significant means of processing and mining a huge amount of biological data due to the ongoing development of high-throughput sequencing technologies.[17] Bioinformatics can also be used to analyze proteins and genomes on a large scale to identify targets

Received: August 8, 2024
Revised: October 25, 2024
Accepted: November 5, 2024
Published: November 9, 2024

associated with disease.[18] Moreover, molecular docking technology represents a theoretical simulation method for studying the interactions between molecules (e.g., drugs and target proteins) and predicting their binding modes and affinities.[19] Combining these two methods can help to identify major drug targets and provide clues for drug development.

To clarify the anticancer mechanism of FCS, this study employed a combination of bioinformatics and molecular docking techniques to screen the main targets of FCS when intervening in LUAD and validated them by experiments.

MATERIALS AND METHODS

Data Acquisition and Differential Expression Analysis. The transcriptome data concerning LUAD, which comprised 541 LUAD tissues and 59 paracancerous tissues, were downloaded from The Cancer Genome Atlas (TCGA) database (https://portal.gdc.cancer.gov/).[20] Data was organized using the R language to remove low-expression genes. Then, quality control was performed, and the expression matrix was analyzed using principal component analysis (PCA). Next, the R language "limma" package was utilized to examine the differences between the tissues.[21] A $P < 0.01$ and |log2(fold change) |>2 were the screening criteria for differentially expressed genes (DEGs). The volcano plots were drawn via the "ggplot2" package.[22]

The DDP-resistant A549 cell data sets, GSE154243 and GSE158638, were downloaded from the Gene Expression Omnibus (GEO) database (https://www.ncbi.nlm.nih.gov/geo/).[23] GSE154243 and GSE158638 each contained one parental and one DDP-resistant A549 cell line. Data quality testing was performed on both GEO data sets using the R language. The matrix data of each data set were normalized and log2 transformed by applying the "limma" package in the R language. The quality of the normalized data met the requirements for subsequent analysis. Next, the fold change (FC) was obtained by taking the difference between the test group (drug-resistant cell lines) and the control group (parental cell lines), and the DEGs were screened using the criteria of FC $\geq 2/\leq 0.5$ or log2|FC| > 2 with $P < 0.05$. Venn diagrams were used to visualize any intersecting genes.

Protein−Protein Interaction (PPI) Network Construction and Analysis. The DEGs were imported into the String online tool (http://www.string-db.org/),[24] and the species was set to "*Homo sapiens*" with a confidence level of 0.9 to obtain the PPI network diagram. In the PPI networks, the nodes represent target proteins, and the edges represent interactions between proteins. Module analysis of PPI networks was performed using the Molecular Complex Detection (MCODE) plug-in for Cytoscape 3.10.0.[25] The MCODE plugin finds the key subnetworks and genes based on the relationship between edges and nodes, and the subnetwork with the highest score is considered to be the core network called "cluster1". Topological analysis of PPI networks was performed using the CytoNCA plug-in. The "Degree", "Betweenness", and "Closeness" scores of the nodes in each network were calculated.[26] After filtering the nodes using the median of these three parameters as a threshold, the nodes were ranked by "Degree", and the top 10 highest-ranked genes were selected as key genes for subsequent analysis.

Survival Analysis. The Kaplan−Meier plotter (http://kmplot.com/analysis)[27] was used to analyze the effect of the gene expression levels on survival in patients with LUAD. The high and low expression groups were categorized according to the median gene expression. A total of 1161 LUAD patients in this database were included in the Kaplan−Meier analysis.

Expression Analysis of Single Genes. Transcriptome data (541 LUAD tissues and 59 normal tissues) downloaded from the TCGA database were used as samples. Differences in the expression of a particular gene between LUAD and normal tissues were analyzed using the "limma" software package.

Functional Enrichment Analysis of the DEGs. The Database for Annotation, Visualization, and Integrated Discovery (DAVID) (https://david.ncifcrf.gov/)[28] was used to perform Gene Ontology (GO) and Kyoto Encyclopedia of Genes and Genomes (KEGG) enrichment analyses. Gene set enrichment analysis (GSEA) is a computational method that determines whether an a priori defined set of genes shows statistically significant, concordant differences between two biological states.[29] GSEA was performed on single genes using GSEA 4.3.2 software and with the C2 gene set as the target. The resulting gene sets were conditionally screened for FCS action, and only those with a false discovery rate (FDR) < 0.05 were considered statistically significant.

Molecular Docking. The two-dimensional (2D) structure of FCS was obtained from the PubChem database (https://pubchem.ncbi.nlm.nih.gov/)[30] and imported into Chem3D 22.0.0 to obtain the three-dimensional (3D) structure. From the Protein Data Bank (PDB) database (https://www.rcsb.org/),[31] the protein structures of polo-like kinase 1 (PLK1, PDB ID:4 × 9R) and budding uninhibited by benzimidazoles 1 (BUB1, PDB ID:5DMZ) were obtained. Pymol 2.5.5 software was then used to perform the required dehydrogenation and primitive ligand removal manipulation.[32] Moreover, molecular docking of FCS to the core target was performed using AutodockTools-1.5.7 software.[33] The optimized molecular structure was subjected to hydrogenation and charge assignment operations to dock the ligand to the receptor active site using semiflexible docking, and the docking results were analyzed. Finally, Pymol 2.5.5 software was used to open the visualized docking results.

Cell Counting Kit-8 (CCK-8) Assay. The logarithmic growth phase cells were gathered, enumerated, and inoculated in 96-well plates at a density of 4×10^3/well. After the cells were attached to the wall, different treatments were provided according to the experimental design and a blank group was established. For the cell proliferation assay, A549 cells and Beas-2B cells (provided by the Central Laboratory of the Affiliated Hospital of Qingdao University, Qingdao, China) were exposed to 0, 10, 50, 100, 200, 500,1000,1500 and 2000 μg/mL FCS (provided by the School of Pharmacy, Ocean University of China, Qingdao, China). For the DDP sensitivity assay, the cells were simultaneously treated with varying doses of DDP (0, 2, 4, 8, 16, and 32 μmol/L; Hansoh Pharma, Jiangsu, China) and 0 or 200 μg/mL FCS. In every group, three duplicate wells were established. At 24 and 48 h after treatment, 10 μL of CCK-8 solution (MedChemExpress, China) was added to each well. The optical density (OD) value at 450 nm was determined using a microplate reader (Thermo Fisher Scientific, USA) after one to 2 h of dark incubation. The cell viability was determined using the following equation: Cell viability = $(OD_{treatment} - OD_{blank})/(OD_{control} - OD_{blank}) \times 100\%$. Moreover, the cell proliferation inhibition rate = 100% − cell viability (%). Based on the proliferation inhibition rate and DDP concentration, the half maximal inhibitory concentration (IC50) value of the DDP

https://doi.org/10.1021/acsomega.4c07295
ACS Omega 2024, 9, 46312−46322

Table 1. Primer Sequences for the qRT-PCR

Genes	Forward	Reverse
BUB1	GAGAAAGCATGAGCAATGGGTAA	GGCAGATCCTCATGGGATGT
PLK1	CCACCAAGGTTTTCGATTGC	GTCGACCACCTCACCTGTCTCT
GADPH	CATGTTCGTCATGGGTGTGAA	GGCATGGACTGTGGTCATGAG

was computed. The experiment was repeated three times independently.

Quantitative Real-Time Polymerase Chain Reaction (qRT-PCR). The logarithmic growth phase A549 cells were gathered. For the cell proliferation assay, there was a control, 200 μg/mL FCS group, and 400 μg/mL FCS group. In terms of the DDP sensitivity assay, there was a control (culture medium only), FCS group (200 μg/mL FCS), DDP group (3 μmol/L DDP), and DDP+FCS group (200 μg/mL FCS+3 μmol/L DDP). Following the various treatments, the cells were cultured for either 24 or 48 h. Next, the growth medium was eliminated and the TRIzol method (Takara Bio, Dalian, China) was used to extract the total RNA on ice. Using the PrimeScript RT Master Mix (Takara Bio, Dalian, China), the cDNA was reverse transcribed. Thermo Fisher Inc. generated the required primer sequences, which are displayed in Table 1. Using a TB Green Premix Ex Taq kit (Takara Bio, Dalian, China) as a guide, the cDNA was used as a template for the qRT-PCR experiments in a LightCycler 480 II Instrument (Roche, Switzerland): predenaturation at 95 °C for 30 s, followed by denaturation at 95 °C for 5 s, annealing at 60 °C for 10 s, and cycling for 40 times. Finally, using GADPH as an internal reference, the $2^{-\Delta\Delta Ct}$ method was used to calculate the relative expression of each gene.

Statistical Analysis. The statistical program GraphPad Prism 6.0 was utilized to quantitatively analyze the data. The data were presented as the mean ± standard deviation. A t test was employed to compare the means of the two samples, while the means of several samples were compared using a one-way analysis of variance (ANOVA). A $P < 0.05$ was considered to be statistically significant.

RESULTS

Identification of the Differentially Expressed Genes (DEGs). As shown in Figure 1A, a total of 692 DEGs, including 326 up-regulated genes and 366 down-regulated genes, were obtained by analyzing the LUAD transcriptome data obtained from the TCGA database. The data sets of the DDP-resistant A549 cells (GSE154243 and GSE158638) were differentially analyzed and the DEGs were derived for each data set independently. Using the DEGs from the two data sets as intersections, a total of 156 up-regulated genes and 251 down-regulated genes were identified (Figure 1B–C), which were used for the subsequent analyses.

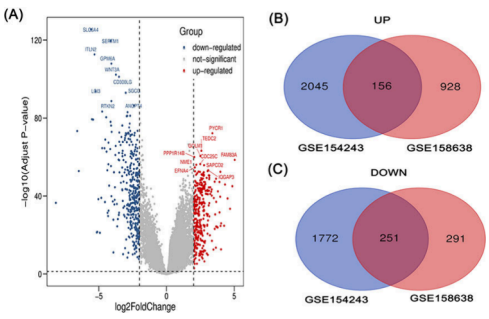

Figure 1. (A) Volcano plot of the LUAD-associated DEGs. Red dots indicate up-regulated DEGs and blue dots indicate down-regulated DEGs. (B–C) Intersection DEGs of the GSE154243 and GSE158638 data sets.

PPI Networks and Module Analysis. PPI networks were created to investigate the interactions between the DEGs, where nodes represent target proteins and edges represent interactions between proteins. There were 691 nodes and 599 edges in the PPI network of the TCGA database (Figure 2A), while 407 nodes and 768 edges in the PPI network of the GEO database (Figure 2C). Then, the PPI network was modularly analyzed using the MCODE plug-in. Pathway enrichment analysis of the modular nodes was performed using DAVID. The TCGA database cluster1 module (score: 16.111) contained 19 genes (Figure 2B), which were enriched in terms of the cell cycle, cellular senescence, P53 signaling route, and FoxO signaling pathway. Moreover, 33 genes (Figure 2D) in the GEO database cluster1 module (score: 14.438) were found to be abundant with regard to the cell cycle, DNA replication, P53 signaling route, and FoxO signaling pathway.

Identifying the Key Genes in the Subnetworks. The topology analysis of the PPI networks was performed using the CytoNCA plugin. After filtering the nodes with the median value of "Degree", "Betweenness", and "Closeness" as the threshold value, the nodes were sorted by "Degree", and the top 10 genes with the highest overall ranking were selected and shown in Table 2.

Survival Analysis. Kaplan–Meier analysis explored the relationship between gene expression and survival in LUAD patients. A total of 9 key targets (PLK1, BUB1, CDK1, CDC20, CCNB1, BUB1B, KIF11, CCNB2, and DLAGP5) obtained from topological analysis were included in this analysis. High expression of seven genes (Figure 3) was linked to a poor prognosis in LUAD patients, which indicates that these genes may serve as prognostic indicators for LUAD. By contrast, CDK1 and BUB1B were not correlated with the prognosis in LUAD patients.

Molecular Docking. Molecular docking was performed to evaluate the interaction between the key targets (7 genes obtained from Kaplan–Meier analysis) and FCS. The binding energy between FCS and targets was obtained by AutoDock software. The better the ligand–receptor binding, the lower its binding energy. Binding energies below −5.0 kcal/mol are generally considered to have good binding activity between ligand and receptor.[34] As shown in Table 3, the molecular docking binding energies of the seven targets were all less than −5, among which the binding energies of PLK1 and BUB1 were less than −8.5, indicating that they are more likely to bind to FCS sufficiently. The docking simulation of FCS with BUB1 and PLK1 is shown in Figure 4.

Characterization of the Target Genes. In this study, PLK1 and BUB1 mRNA expression was analyzed in lung cancer tissues using the TCGA database. Figure 5A shows a 30-fold increase in PLK1 and BUB1 expression in the tumor tissues compared to normal tissue ($p < 0.001$). Next, GSEA

https://doi.org/10.1021/acsomega.4c07295
ACS Omega 2024, 9, 46312–46322

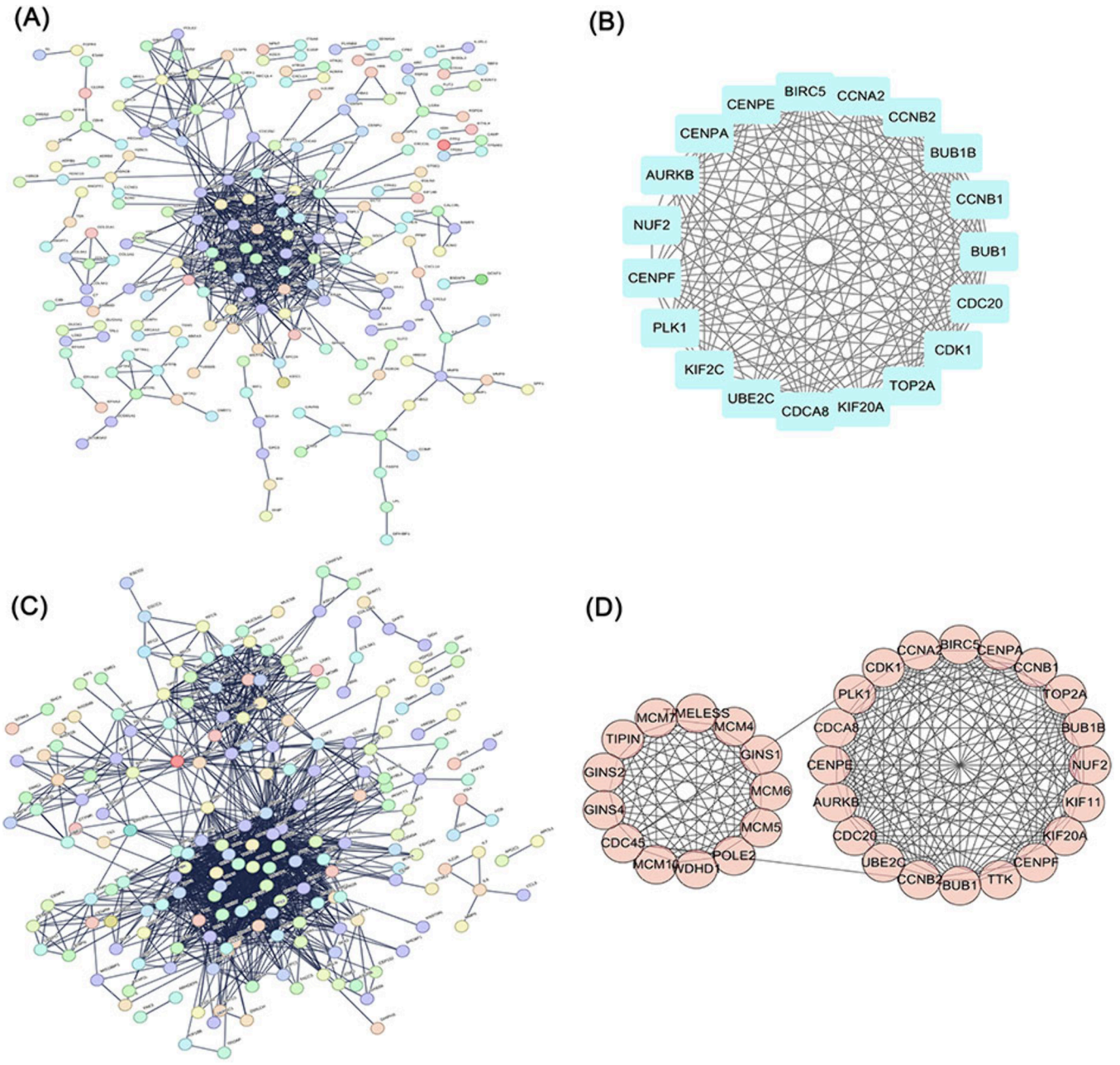

Figure 2. (A) PPI network of the DEGs in the TCGA database. (B) The core module of the TCGA PPI network, cluster1, contained 19 genes. (C) PPI network of the DEGs in the GEO database. (D) The core module of the GEO PPI network, cluster1, contained 33 genes.

analysis was used to analyze individual genes' relevance and regulatory mechanisms to LUAD. The results showed that both BUB1 and PLK1 were enriched in the P53 signaling pathway (Figure 5B). As a result, BUB1 and PLK1 were chosen as the key targets for further experimental confirmation.

Effect of FCS on Cell Viability. The cell viability following FCS treatment at different concentrations (0, 10, 50, 100, 200, 500, 1000, 1500, and 2000 μg/mL) was determined via the CCK-8 method. The vitality of the A549 cells declined with increasing concentration, as demonstrated in Figure 6A. After 24 h of treatment at 500, 1000, 1500, and 2000 μg/mL concentrations, the cell viability of A549 cells was statistically different from that of the control group ($P < 0.05$). Nevertheless, the proliferation inhibitory effect of FCS on the Beas-2B cells was not obvious ($P > 0.05$). As shown in Figure 6B, the cell viability of A549 cells treated with 100, 200, 500, 1000, 1500, and 2000 μg/mL FCS for 48h showed statistically significant differences compared with the control ($P < 0.05$). Moreover, there was no difference in cell viability of the same concentration treated for 24h or 48h ($P > 0.05$). Based on these findings, it is proposed that FCS might, in a dose-dependent manner, suppress the growth of A549 cells.

Effect of FCS on DDP Sensitivity. As shown in Figure 7, the combination of 200 μg/mL FCS and different concentrations (0, 2, 4, 8, 16, and 32 μmol/L) of DDP had greater inhibitory effects on cell viability than DDP alone ($P < 0.05$). In addition, FCS enhanced the DDP sensitivity of the A549 cells, as evidenced by the lower IC50 values. The IC50 value after 24h of treatment was (4.015 ± 0.255) μmol/L in the combined group and (5.044 ± 0.306) μmol/L in the DDP

https://doi.org/10.1021/acsomega.4c07295
ACS Omega 2024, 9, 46312−46322

Table 2. Top 10 Most Dominant Genes in the PPI Networks from the TCGA and GEO Databases[a]

	TCGA database				GEO database			
ID	Gene	Degree	Betweenness	Closeness	Gene	Degree	Betweenness	Closeness
1	CDK1	44	2117.6287	0.008988663	CDK1	48	7155.6924	0.034746762
2	CDC20	36	330.96606	0.008980955	CDC20	39	884.51337	0.03435559
3	BUB1	36	349.3952	0.008981765	CCNB1	39	791.39233	0.034422405
4	BUB1B	35	442.25946	0.008980955	BUB1B	35	1467.4622	0.0343356
5	CCNB1	33	208.46059	0.00898055	KIF11	35	1328.6719	0.034255855
6	DLGAP5	33	350.7342	0.008976904	BUB1	34	519.6512	0.03434226
7	KIF11	32	538.9637	0.008976499	CCNB2	33	1933.9503	0.0344962
8	CENPF	30	390.79608	0.008978119	DLGAP5	33	476.01373	0.034229357
9	CCNB2	29	657.57544	0.00898136	PLK1	31	2746.4983	0.034382284
10	PLK1	26	565.2614	0.008976499	CCNA2	30	1449.8549	0.034382284

[a]A total of nine genes were found to be significant in both databases, suggesting that these genes may be associated with DDP resistance and LUAD. These genes were protein structures of polo-like kinase 1 (PLK1), budding uninhibited by benzimidazoles 1 (BUB1), cyclin-dependent kinase 1 (CDK1), cell division cycle 20 (CDC20), cyclin B1 (CCNB1), BUB1 mitotic checkpoint serine/threonine kinase B (BUB1B), kinesin family member 11 (KIF11), cyclin B2 (CCNB2), and DLG-associated protein 5 (DLAGP5).

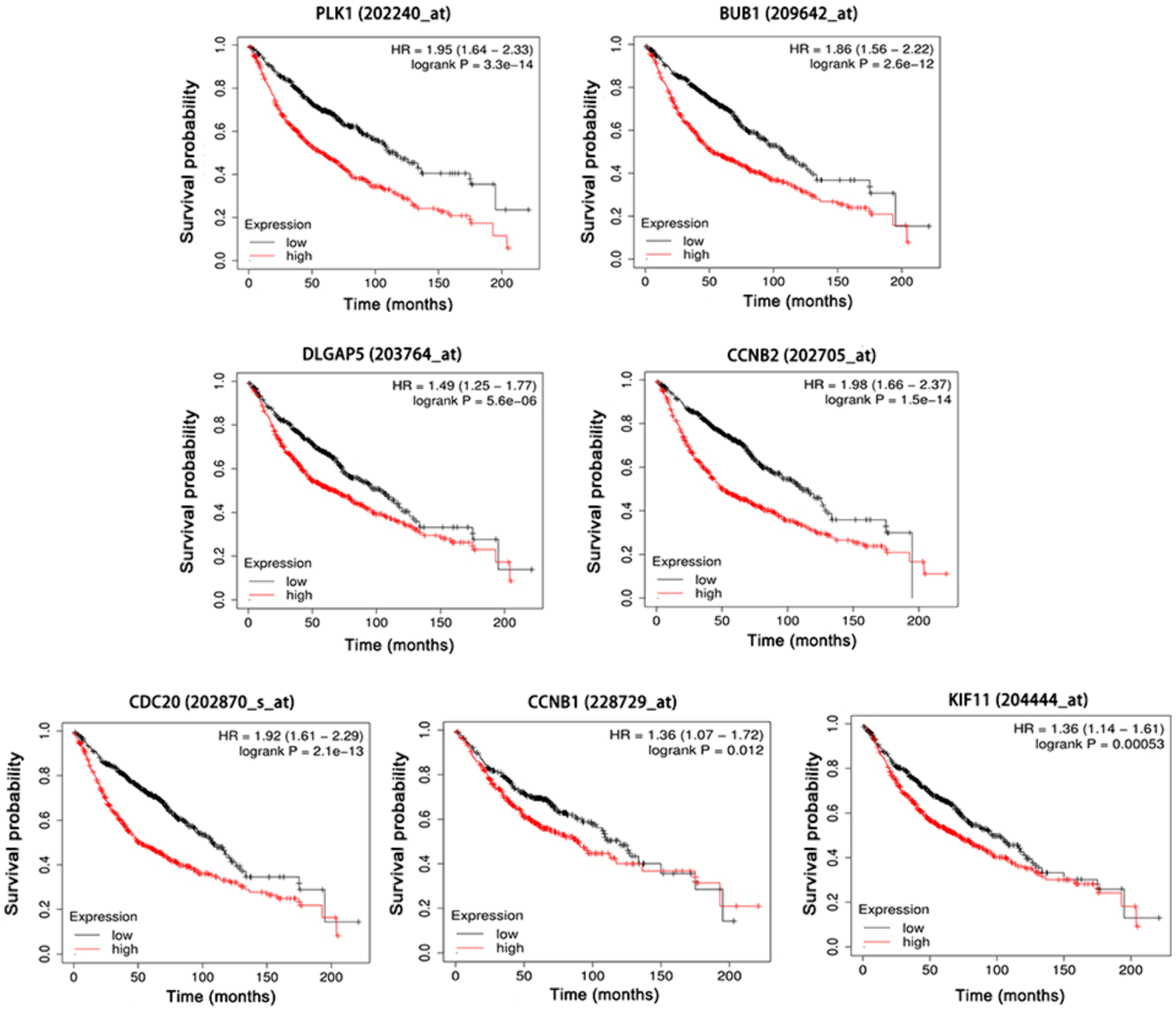

Figure 3. Kaplan–Meier curves of seven prognostically relevant genes in LUAD. The red line represents patients with high gene expression, and the black line represents patients with low gene expression. Hazard Ratio (HR) > 1 and $P < 0.05$, suggesting that patients with high gene expression had worse survival than patients with low gene expression.

https://doi.org/10.1021/acsomega.4c07295
ACS Omega 2024, 9, 46312–46322

Table 3. Molecular Docking Binding Energy of Each Target

Protein	PDB ID	Binding energy(kcal/mol)
PLK1	4X9R	−10.19
BUB1	5dmz	−8.96
CCNB2	2CCH	−8.26
KIF11	3ZCW	−8.01
CDC20	4GGC	−7.3
CCNB1	5LQF	−7.25
DLGAP5	7ZX4	−5.11

group, which was statistically different between the two groups ($P < 0.05$). Similarly, the IC50 value was (2.279 ± 0.373) μmol/L in the combined group after 48h of treatment, which was statistically different compared to (3.187 ± 0.289) μmol/L in the DDP group ($P < 0.05$).

BUB1 and PLK1 mRNA Expression in FCS-Treated Cells. The qRT-PCR technique was used to confirm that BUB1 and PLK1 mRNA were expressed following FCS treatment. As shown in Figure 8, the expression of both BUB1 and PLK1 mRNA in the FCS-treated A549 cells was significantly inhibited in a dose- and time-dependent manner, which suggests that FCS may inhibit the proliferation of A549 cells by suppressing the expression of BUB1 and PLK1 mRNA. This accords with the results of the bioinformatics analysis.

Based on the above results, 200 μg/mL FCS and 3 μmol/L DDP were selected for further experimental validation. As shown in Figure 9, the expression of both PLK1 and BUB1 mRNA was decreased in the DDP+FCS group when compared with the control, DDP, and FCS groups, with the difference being statistically significant ($P < 0.05$). This suggests that the combination of DDP and FCS could significantly inhibit the expression of BUB1 and PLK1 mRNA to exert the DDP-sensitizing effect, which is in agreement with the results of the bioinformatics analysis.

DISCUSSION

LUAD is the most prevalent pathologic type of lung cancer.[35] Moreover, the five-year mortality rate of LUAD patients, depending on the stage, ranges from 43% to 95%.[36] DDP is commonly used in the treatment of advanced LUAD and as an adjuvant chemotherapy agent.[37] However, this treatment can lead to resistance in malignant cells, which is one of the reasons for treatment failure in LUAD, resulting in tumor

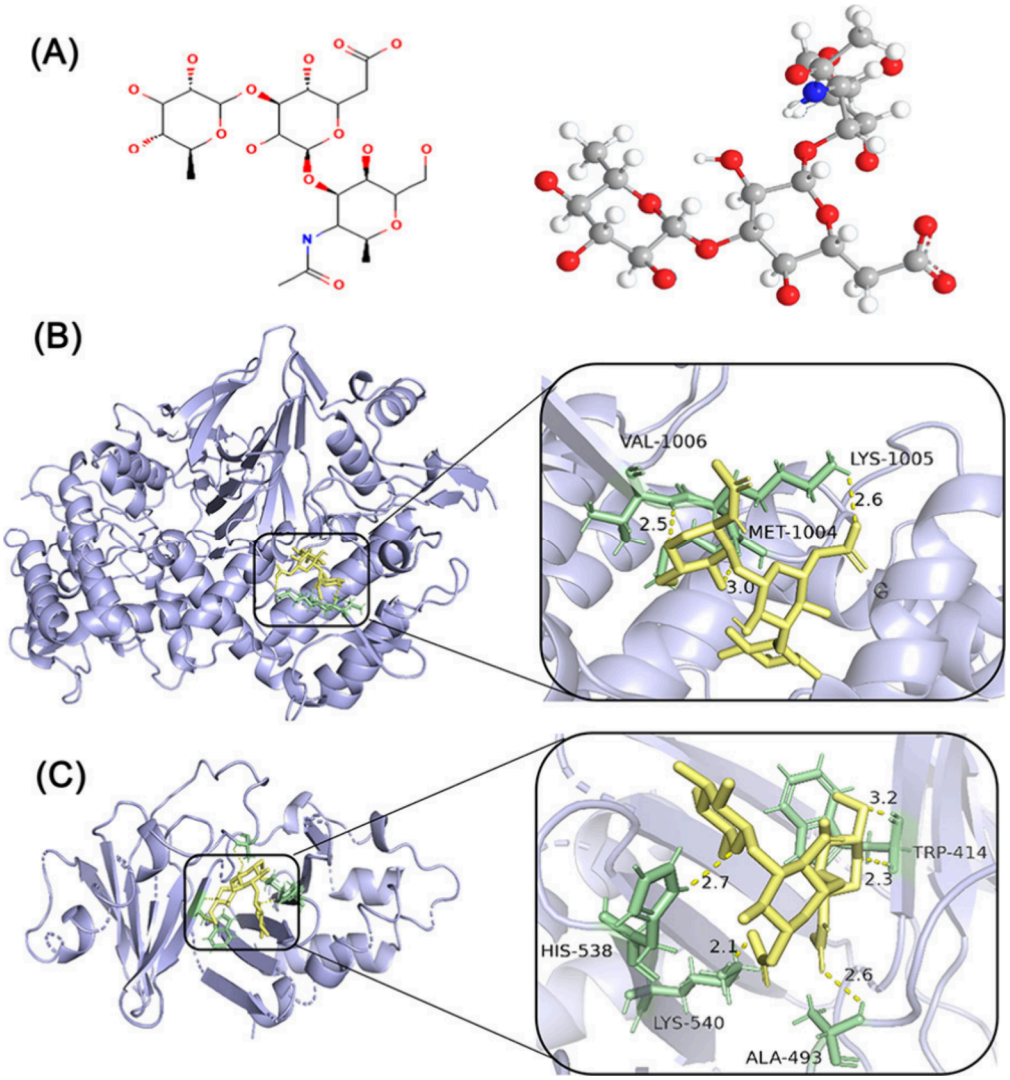

Figure 4. Molecular docking model of the key targets. (A) 2D (left) and 3D (right) structures of FCS. The yellow structure represents FCS, while the green structure represents the binding sites of FCS with BUB1 (B) and PLK1 (C).

https://doi.org/10.1021/acsomega.4c07295
ACS Omega 2024, 9, 46312−46322

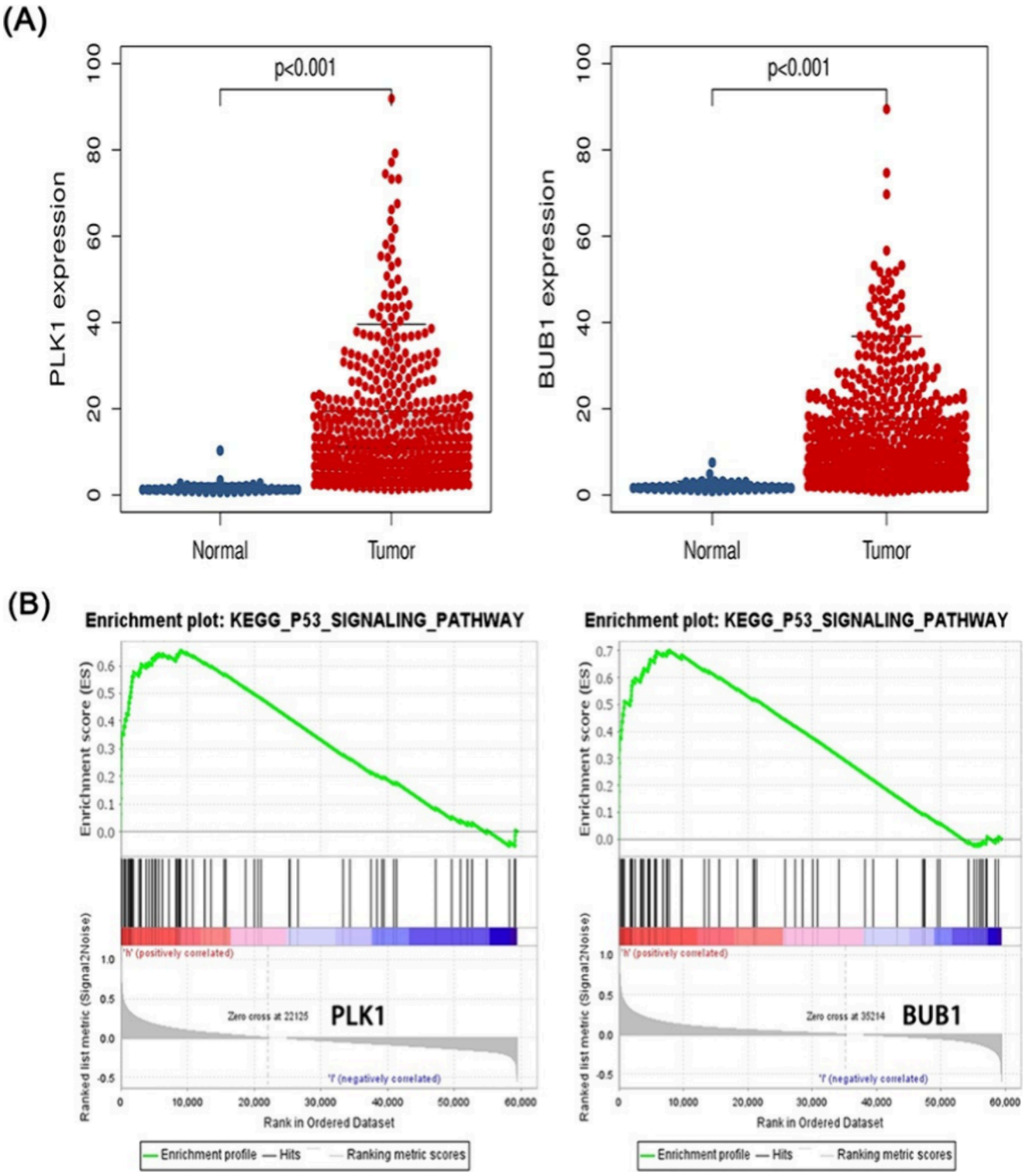

Figure 5. (A) Expression of PLK1 and BUB1 in LUAD tissues. With a $p < 0.001$, a significant difference was found when compared with the normal samples. (B) GSEA enrichment analysis of PLK1 and BUB1.

recurrence and disease progression.[38] Thus, an urgent issue associated with the treatment of LUAD is the development of effective treatments.

Natural medicines have been used for centuries to treat various diseases due to their novel structure, high activity, and low adverse effects.[39] Studying the targets of natural drugs is important when it comes to exploring the related therapeutic mechanisms.[40,41] Bioinformatics plays an irreplaceable role in the discovery of drug targets and is particularly suitable for the analysis of large-scale multiomics data.[42] Furthermore, molecular docking is one of the most favored and effective structure-based computer simulation methods, helping to predict the interactions between molecules and biological targets.[43] To accomplish this, a tiny molecule (ligand) is placed in the binding region of a big molecule target (receptor) and

https://doi.org/10.1021/acsomega.4c07295
ACS Omega 2024, 9, 46312−46322

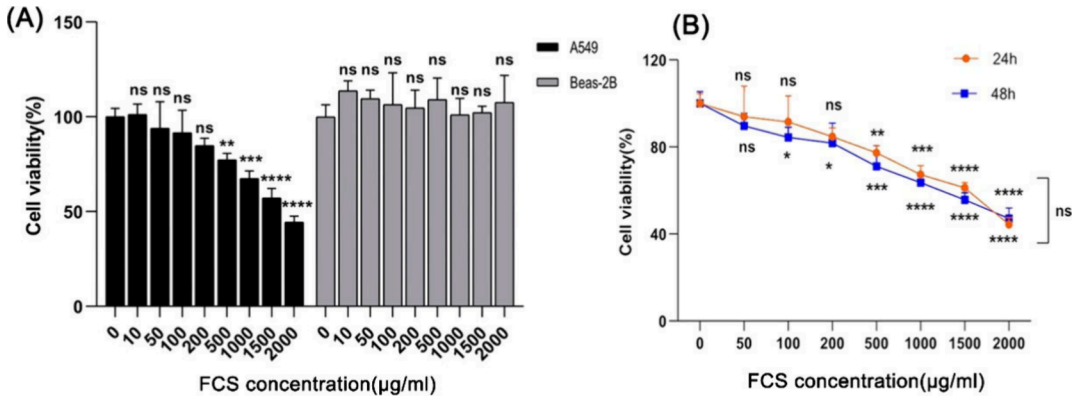

Figure 6. Cell viability after FCS treatment. (A) Cell viability after 24 h of treatment with different concentrations of FCS. (B) Cell viability after different concentrations of FCS treatment for 24 and 48 h. * $P < 0.05$, ** $P < 0.01$, *** $P < 0.001$, **** $P < 0.0001$.

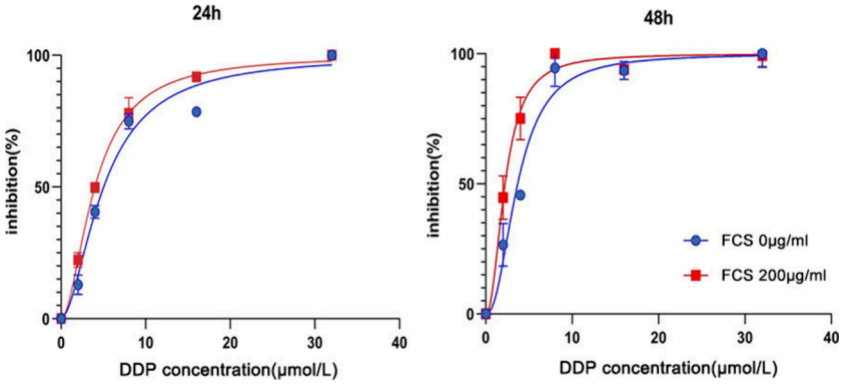

Figure 7. Cell proliferation inhibition rate after cotreatment with different concentrations of DDP and FCS.

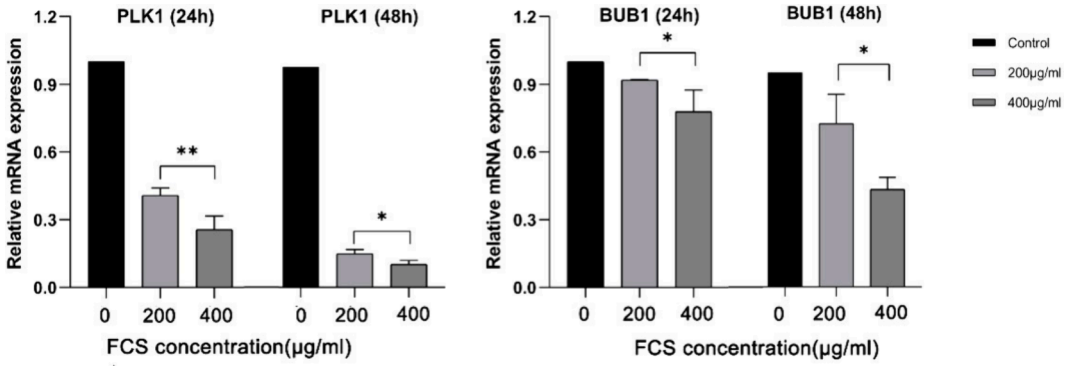

Figure 8. Expression of PLK1 and BUB1 mRNA in A549 cells following treatment with different concentrations of FCS. * $P < 0.05$, ** $P < 0.01$.

the physicochemical characteristics are calculated to estimate the binding force and binding mode of the two molecules.[44]

FCS, one of the primary active components of a sea cucumber's body wall,[45] is a branched heteropolysaccharide with a relative molecular mass of 40,000−50,000, consisting of N-Acetyl-D-galactosamine hydrate, D-glucuronic acid, and L-fucose.[46] It has been reported that FCS may have inhibitory effects on the spread and growth of tumors.[47] FCS derived from *Isostichopus badionotus* significantly decreases the migration, invasion, and adhesion of human lung cancer 95D cells in a dose-dependent way.[48] Liu et al. discovered that FCS slows the proliferation of Lewis lung cancer cells, which might be related to Caspase-3-induced apoptosis.[49] In the present study, FCS inhibited the growth of human LUAD A549 cells in a dose-dependent manner and also enhanced the sensitivity of A549 cells to DDP. Afterward, based on bioinformatics analysis and molecular docking, it was discovered that the intervention of FCS in relation to LUAD might be related to the BUB1 and PLK1 genes.

PLK1 is a serine/threonine protein kinase widespread in eukaryotic cells that is mainly engaged in cell cycle regulation and cancer.[50] Genetic repression of PLK1 leads to abnormal chromosome segregation, resulting in mitotic arrest, usually accompanied by cell death.[51] PLK1 is frequently overexpressed in a variety of tumor types and linked to unfavorable clinical outcomes.[52] Consistent with previous findings, this study found that patients with LUAD who exhibited high PLK1 expression had a worse prognosis. Furthermore, prior studies have shown that PLK1 inhibition increases the susceptibility of cancer cells to both chemotherapy and radiation, while PLK1

https://doi.org/10.1021/acsomega.4c07295
ACS Omega 2024, 9, 46312−46322

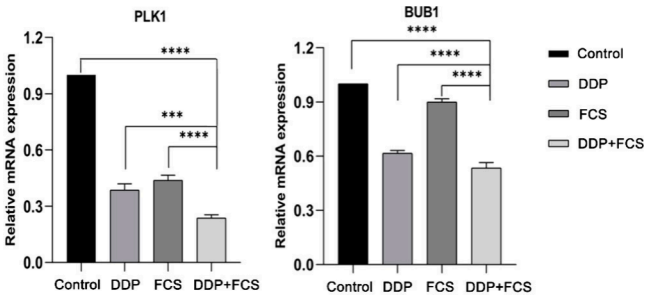

Figure 9. PLK1 and BUB1 mRNA expression in A549 cells after 24 h of different treatments. There was a control group, DDP group (3 μmol/L), FCS group (200 μg/mL), and DDP+FCS group (200 μg/mL FCS+3 μmol/L DDP). When compared with the other groups, the DDP+FCS group's BUB1 and PLK1 mRNA expression was statistically significant. *** $P < 0.001$, **** $P < 0.0001$.

overexpression is linked to chemoresistance.[53] BUB1 is a cell cycle protein with an N-terminal end that binds to kinetochores and thus plays a crucial role in mitosis.[54] BUB1 plays an important role in a variety of cancers, including breast, ovarian, and colon cancers.[55] In human LUAD A549 cells, this study confirmed that FCS could decrease the expression of both PLK1 and BUB1 mRNA. The down-regulation of PLK1 and BUB1 mRNA was more noticeable when FCS was combined with DDP. This finding is in keeping with the expected outcomes and suggests that BUB1 and PLK1 might be the targets of FCS intervention in LUAD.

Accordingly, this study showed that both BUB1 and PLK1 were significantly up-regulated in the LUAD tissues when compared with normal tissues. High expression of these two genes was linked to a poor prognosis in LUAD patients, which indicates that these genes may serve as prognostic indicators for LUAD. FCS had no inhibitory effect on normal lung epithelial cells but could inhibit the growth of human LUAD cells and enhance the sensitivity of LUAD cells to DDP by inhibiting the expression of PLK1 and BUB1. Thus, FCS could be considered a potent LUAD inhibitor and a potential chemosensitizer. In addition, these findings imply that molecular docking and bioinformatics analysis perform effectively together to anticipate natural compounds' potential therapeutic targets.

However, this study also has some limitations. First, we only performed experiments with normal lung epithelial cells and human LUAD cells to validate the identified targets. Second, the signaling pathways regulated by the target genes were not explored. Third, more pharmacological studies are also needed to determine the optimal dose and bioavailability of FCS. Therefore, we will conduct high-quality animal experiments and explore the signaling pathways regulated by the target genes in the next phase to provide an exact molecular mechanism for the application of FCS in LUAD therapy.

CONCLUSIONS

BUB1 and PLK1 might be the primary genes in involved in FCS's regulation of LUAD cell growth and susceptibility to DDP. In addition, combined molecular docking and bioinformatics analysis could effectively predict natural compounds' potential therapeutic targets.

AUTHOR INFORMATION

Corresponding Author

Cunzhi Lin − *Department of Respiratory and Critical Care Medicine, The Affiliated Hospital of Qingdao University, Qingdao 266003, China*; Email: lindoc@126.com

Authors

Nana Li − *Department of Respiratory and Critical Care Medicine, The Affiliated Hospital of Qingdao University, Qingdao 266003, China*; orcid.org/0000-0003-2882-7045

Xinhong Zhu − *Department of International Medicine, Qingdao Municipal Hospital Group, Qingdao 266071, China*

Hua Zhang − *Department of Respiratory and Critical Care Medicine, The Affiliated Hospital of Qingdao University, Qingdao 266003, China*

Xiaohui Yang − *Department of Respiratory and Critical Care Medicine, The Affiliated Hospital of Qingdao University, Qingdao 266003, China*

Mingju Shao − *Department of Respiratory and Critical Care Medicine, The Affiliated Hospital of Qingdao University, Qingdao 266003, China*

Shichao Cui − *Department of Respiratory and Critical Care Medicine, The Affiliated Hospital of Qingdao University, Qingdao 266003, China*

Complete contact information is available at: https://pubs.acs.org/10.1021/acsomega.4c07295

Notes

The authors declare no competing financial interest.

ACKNOWLEDGMENTS

The author(s) disclosed receipt of the following financial support for the research, authorship, and/or publication of this article: This project was supported by the Key Laboratory of Marine Drug, Ministry of Education (KLMDOUC201307).

REFERENCES

(1) Thai, A. A.; Solomon, B. J.; Sequist, L. V.; Gainor, J. F.; Heist, R. S. Lung cancer. *Lancet* **2021**, *398* (10299), 535−554.

(2) Hirsch, F. R.; Scagliotti, G. V.; Mulshine, J. L.; et al. Lung cancer: current therapies and new targeted treatments. *Lancet* **2017**, *389* (10066), 299−311.

(3) Duma, N.; Santana-Davila, R.; Molina, J. R. Non−Small Cell Lung Cancer: Epidemiology, Screening, Diagnosis, and Treatment. *Mayo Clinic Proceedings* **2019**, *94* (8), 1623−1640.

(4) Lambe, G.; Durand, M.; Buckley, A.; Nicholson, S.; McDermott, R. Adenocarcinoma of the lung: from BAC to the future. *Insights Imaging* **2020**, *11* (1), 69.

(5) Arbour, K. C.; Riely, G. J. Systemic Therapy for Locally Advanced and Metastatic Non−Small Cell Lung Cancer: A Review. *JAMA* **2019**, *322* (8), 764.

(6) Zhang, C.; Xu, C.; Gao, X.; Yao, Q. Platinum-based drugs for cancer therapy and anti-tumor strategies. *Theranostics* **2022**, *12* (5), 2115−2132.

(7) Atanasov, A. G.; Zotchev, S. B.; Dirsch, V. M.; Supuran, C. T. Natural products in drug discovery: advances and opportunities. *Nat. Rev. Drug Discovery* **2021**, *20* (3), 200.

(8) Dutta, S.; Mahalanobish, S.; Saha, S.; Ghosh, S.; Sil, P. C. Natural products: An upcoming therapeutic approach to cancer. *Food and chemical toxicology: an international journal published for the British Industrial Biological Research Association* **2019**, *128*, 240.

https://doi.org/10.1021/acsomega.4c07295
ACS Omega 2024, 9, 46312−46322

(9) Hossain, A.; Dave, D.; Shahidi, F. Sulfated polysaccharides in sea cucumbers and their biological properties: A review. *Int. J. Biol. Macromol.* **2023**, *253*, No. 127329.
(10) Ustyuzhanina, N. E.; Bilan, M. I.; Anisimova, N. Y.; et al. Depolymerization of a fucosylated chondroitin sulfate from Cucumaria japonica: Structure and activity of the product. *Carbohydr. Polym.* **2022**, *281*, No. 119072.
(11) Xu, H.; Zhou, Q.; Liu, B.; Chen, F.; Wang, M. Holothurian fucosylated chondroitin sulfates and their potential benefits for human health: Structures and biological activities. *Carbohydr. Polym.* **2022**, *275*, No. 118691.
(12) Lin, C.; Zhu, X.; Jin, Q.; Sui, A.; Li, J.; Shen, L. Effects of Holothurian Glycosaminoglycan on the Sensitivity of Lung Cancer to Chemotherapy. *Integr Cancer Ther.* **2020**, *19*, No. 1534735420911430.
(13) Mukherjee, P.; Zhou, X.; Benicky, J.; et al. Heparan-6-O-Endosulfatase 2 Promotes Invasiveness of Head and Neck Squamous Carcinoma Cell Lines in Co-Cultures with Cancer-Associated Fibroblasts. *Cancers (Basel)* **2023**, *15* (21), 5168.
(14) Zhou, L.; Yin, R.; Gao, N.; et al. Oligosaccharides from fucosylated glycosaminoglycan prevent breast cancer metastasis in mice by inhibiting heparanase activity and angiogenesis. *Pharmacol. Res.* **2021**, *166*, No. 105527.
(15) Liu, Y.; Liu, X.; Ye, Q.; et al. Fucosylated Chondroitin Sulfate against Parkinson's Disease through Inhibiting Inflammation Induced by Gut Dysbiosis. *J. Agric. Food Chem.* **2022**, *70* (42), 13676−13691.
(16) Yin, R.; Pan, Y.; Cai, Y.; et al. Re-understanding of structure and anticoagulation: Fucosylated chondroitin sulfate from sea cucumber Ludwigothurea grisea. *Carbohydr. Polym.* **2022**, *294*, No. 119826.
(17) He, H.; Duo, H.; Hao, Y.; et al. Computational drug repurposing by exploiting large-scale gene expression data: Strategy, methods and applications. *Comput. Biol. Med.* **2023**, *155*, No. 106671.
(18) Huang, Y. Q.; Sun, P.; Chen, Y.; Liu, H. X.; Hao, G. F.; Song, B. A. Bioinformatics toolbox for exploring target mutation-induced drug resistance. *Brief Bioinform.* **2023**, *24* (2), No. bbad033.
(19) Pinzi, L.; Rastelli, G. Molecular Docking: Shifting Paradigms in Drug Discovery. *Int. J. Mol. Sci.* **2019**, *20* (18), 4331.
(20) Grossman, R. L.; Heath, A. P.; Ferretti, V.; et al. Toward a Shared Vision for Cancer Genomic Data. *N Engl J. Med.* **2016**, *375* (12), 1109−1112.
(21) Ritchie, M. E.; Phipson, B.; Wu, D.; et al. limma powers differential expression analyses for RNA-sequencing and microarray studies. *Nucleic Acids Res.* **2015**, *43* (7), No. e47.
(22) Wickham, H *ggplot2: Elegant Graphics for Data Analysis*; Springer-Verlag: New York, 2016:, https://ggplot2.tidyverse.org.
(23) Barrett, T.; Wilhite, S. E.; Ledoux, P.; Evangelista, C.; Kim, I. F.; Tomashevsky, M.; Marshall, K. A.; Phillippy, K. H.; Sherman, P. M.; Holko, M.; et al. NCBI GEO: archive for functional genomics data sets–update. *Nucleic Acids Res.* **2012**, *41*, D991−995.
(24) Szklarczyk, D.; Kirsch, R.; Koutrouli, M.; et al. The STRING database in 2023: protein-protein association networks and functional enrichment analyses for any sequenced genome of interest. *Nucleic Acids Res.* **2023**, *51* (D1), D638−D646.
(25) Bader, G. D.; Hogue, C. W. V. An automated method for finding molecular complexes in large protein interaction networks. *BMC Bioinformatics* **2003**, *4*, 2.
(26) Tang, Y.; Li, M.; Wang, J.; Pan, Y.; Wu, F. X. CytoNCA: A cytoscape plugin for centrality analysis and evaluation of protein interaction networks. *Biosystems* **2015**, *127*, 67−72.
(27) Győrffy, B. Integrated analysis of public datasets for the discovery and validation of survival-associated genes in solid tumors. *Innovation (Camb)* **2024**, *5* (3), No. 100625.
(28) Sherman, B. T.; Hao, M.; Qiu, J.; et al. DAVID: a web server for functional enrichment analysis and functional annotation of gene lists (2021 update). *Nucleic Acids Res.* **2022**, *50* (W1), W216−W221.
(29) Subramanian, A.; Tamayo, P.; Mootha, V. K.; et al. Gene set enrichment analysis: a knowledge-based approach for interpreting genome-wide expression profiles. *Proc. Natl. Acad. Sci. U. S. A.* **2005**, *102* (43), 15545−15550.
(30) Kim, S.; Chen, J.; Cheng, T.; et al. PubChem 2023 update. *Nucleic Acids Res.* **2023**, *51* (D1), D1373−D1380.
(31) Burley, S. K.; Bhikadiya, C.; Bi, C.; et al. RCSB Protein Data Bank (RCSB.org): delivery of experimentally-determined PDB structures alongside one million computed structure models of proteins from artificial intelligence/machine learning. *Nucleic Acids Res.* **2023**, *51* (D1), D488−D508.
(32) DeLano, W. L. *PyMOL Molecular Graphics System*; Schrödinger, 2002; http://www.pymol.org.
(33) Forli, S.; Huey, R.; Pique, M. E.; Sanner, M. F.; Goodsell, D. S.; Olson, A. J. Computational protein-ligand docking and virtual drug screening with the AutoDock suite. *Nat. Protoc.* **2016**, *11* (5), 905−919.
(34) Abdalfattah, S.; Knorz, C.; Ayoobi, A.; et al. Identification of Antagonistic Action of Pyrrolizidine Alkaloids in Muscarinic Acetylcholine Receptor M1 by Computational Target Prediction Analysis. *Pharmaceuticals (Basel)* **2024**, *17* (1), 80.
(35) Chen, P.; Liu, Y.; Wen, Y.; Zhou, C. Non-small cell lung cancer in China. *Cancer Commun. (Lond)* **2022**, *42* (10), 937−970.
(36) Seguin, L.; Durandy, M.; Feral, C. C. Lung Adenocarcinoma Tumor Origin: A Guide for Personalized Medicine. *Cancers (Basel)* **2022**, *14* (7), 1759.
(37) Ghosh, S. Cisplatin: The first metal based anticancer drug. *Bioorganic Chemistry* **2019**, *88*, No. 102925.
(38) Zhang, Y.; Chang, D.; Zhang, J. Research Advances in Resistance to Platinum-based Chemotherapy in Lung Cancer. *Zhongguo Yi Xue Ke Xue Yuan Xue Bao* **2017**, *39* (1), 150−155.
(39) Tewari, D.; Rawat, P.; Singh, P. K. Adverse drug reactions of anticancer drugs derived from natural sources. *Food Chem. Toxicol.* **2019**, *123*, 522−535.
(40) Dasari, S.; Njiki, S.; Mbemi, A.; Yedjou, C. G.; Tchounwou, P. B. Pharmacological Effects of Cisplatin Combination with Natural Products in Cancer Chemotherapy. *International journal of molecular sciences* **2022**, *23* (3), 1532.
(41) Hashem, S.; Ali, T. A.; Akhtar, S.; Nisar, S.; Sageena, G.; Ali, S.; Al-Mannai, S.; Therachiyil, L.; Mir, R.; Elfaki, I. Targeting cancer signaling pathways by natural products: Exploring promising anti-cancer agents. *Biomedicine & pharmacotherapy* **2022**, *150*, 113054.
(42) Zhang, Y.; Luo, M.; Wu, P.; Wu, S.; Lee, T. Y.; Bai, C. Application of Computational Biology and Artificial Intelligence in Drug Design. *Int. J. Mol. Sci.* **2022**, *23* (21), 13568.
(43) Kaur, T.; Madgulkar, A.; Bhalekar, M.; Asgaonkar, K. Molecular Docking in Formulation and Development. *Curr. Drug Discov Technol.* **2019**, *16* (1), 30−39.
(44) Stanzione, F.; Giangreco, I.; Cole, J. C. Use of molecular docking computational tools in drug discovery. *Prog. Med. Chem.* **2021**, *60*, 273−343.
(45) Zhang, L.; Xu, P.; Liu, B.; Yu, B. Chemical Synthesis of Fucosylated Chondroitin Sulfate Oligosaccharides. *J. Org. Chem.* **2020**, *85* (24), 15908−15919.
(46) Shi, D.; Qi, J.; Zhang, H.; Yang, H.; Yang, Y.; Zhao, X. Comparison of hydrothermal depolymerization and oligosaccharide profile of fucoidan and fucosylated chondroitin sulfate from Holothuria floridana. *Int. J. Biol. Macromol.* **2019**, *132*, 738−747.
(47) Li, J.; Li, S.; Wu, L.; et al. Ultrasound-assisted fast preparation of low molecular weight fucosylated chondroitin sulfate with antitumor activity. *Carbohydr. Polym.* **2019**, *209*, 82−91.
(48) He, M.; Wang, J.; Hu, S.; Wang, Y.; Xue, C.; Li, H. The effects of fucosylated chondroitin sulfate isolated from Isostichopus badionotus on antimetastatic activity via down-regulation of Hif-1 alpha and Hpa. *Food Sci. Biotechnol.* **2014**, *23* (5), 1643−1651.
(49) Liu, X.; Liu, Y.; Hao, J.; et al. In Vivo Anti-Cancer Mechanism of Low-Molecular-Weight Fucosylated Chondroitin Sulfate (LFCS) from Sea Cucumber Cucumaria frondosa. *Molecules.* **2016**, *21* (5), 625.

https://doi.org/10.1021/acsomega.4c07295
ACS Omega 2024, 9, 46312−46322

(50) Iliaki, S.; Beyaert, R.; Afonina, I. S. Polo-like kinase 1 (PLK1) signaling in cancer and beyond. *Biochem. Pharmacol.* **2021**, *193*, No. 114747.
(51) Kim, T. Recent Progress on the Localization of PLK1 to the Kinetochore and Its Role in Mitosis. *Int. J. Mol. Sci.* **2022**, *23* (9), 5252.
(52) Chiappa, M.; Petrella, S.; Damia, G.; Broggini, M.; Guffanti, F.; Ricci, F. Present and Future Perspective on PLK1 Inhibition in Cancer Treatment. *Front Oncol.* **2022**, *12*, No. 903016.
(53) Su, S.; Chhabra, G.; Singh, C. K.; Ndiaye, M. A.; Ahmad, N. PLK1 inhibition-based combination therapies for cancer management. *Transl Oncol.* **2022**, *16*, No. 101332.
(54) Elowe, S.; Bolanos-Garcia, V. M. The spindle checkpoint proteins BUB1 and BUBR1: (SLiM)ming down to the basics. *Trends Biochem. Sci.* **2022**, *47* (4), 352−366.
(55) Kim, T.; Gartner, A. Bub1 kinase in the regulation of mitosis. *Anim Cells Syst. (Seoul)* **2021**, *25* (1), 1−10.

https://doi.org/10.1021/acsomega.4c07295
ACS Omega 2024, 9, 46312−46322